エッジ重みの不確実性に対して頑健なインフィマル畳み込み型グラフ正則化

Robust Infimal Convolutional Graph Regularization Against Edge Weight Uncertainty

月足友音　　　　　　小野峻佑
東京科学大学

Yuto TSUKIASHI　　　　　　Shunsuke ONO
Institute of Science Tokyo

Abstract　Graph signal recovery is a central task in graph signal processing, with applications across diverse networked data domains. Graph Laplacian regularization (GLR) is a well-established approach for smooth signal recovery, but it heavily relies on an assumption that rarely holds: edge weights accurately reflect signal characteristics. Graph total variation (GTV) offers more robustness to weight uncertainties but under-penalizes small differences on reliable edges, limiting its effectiveness. We propose a novel infimal convolution–based regularizer that adaptively combines the strengths of GLR and GTV. Reliable edges with small signal differences are effectively handled by the quadratic component, while unreliable edges with larger differences are better explained by the ℓ_1 component. This mechanism enables robust recovery in the presence of edge weight uncertainties without sacrificing performance when weights are accurate. We formulate recovery as a convex optimization problem and develop an efficient solver via a pre-conditioned primal–dual splitting method. Experiments on graph signal recovery with perturbed edge weights show that our approach consistently outperforms GLR and GTV, achieving robust and accurate recovery under uncertainty.

1　Introduction

Graph Signal Processing (GSP) provides a powerful framework for extending classical signal processing concepts to data residing on irregular domains represented by graphs [1–4]. This perspective has enabled principled methods for analyzing and processing a wide variety of network-structured data, with applications ranging from sensor networks and transportation systems to neuroscience and social media analysis.

Among various problems studied in this field, *graph signal recovery*—the recovery of signals defined on graph nodes from noisy, missing, or corrupted observations—is one of the most fundamental tasks. Accurate and efficient recovery is critical not only as a stand-alone problem, but also as a building block for downstream tasks such as classification, clustering, and learning over graphs. Consequently, a large body of research has been devoted to this topic [5–10].

Among various approaches to (undirected) graph signal recovery, one of the most widely used methods is graph Laplacian regularization (GLR) [11,12], which is designed for smooth graph signals. In simple denoising settings, this regularization admits a closed-form solution that can be interpreted as graph filtering [13,14]. In more advanced recovery problems, it typically leads to convex optimization formulations [15], which can be efficiently solved using proximal splitting methods [16,17].

A key premise behind GLR is that the given edge weights of the graph accurately reflect the underlying structure of the signal. In practice, however, this assumption rarely holds. Even when the graph topology is partially known, assigning accurate edge weights that capture the true similarity between nodes is notoriously difficult. When the graph itself is learned from data, uncertainties in edge weights become even more pronounced. For these reasons, the effectiveness of GLR is highly sensitive to inaccuracies in the graph structure.

An alternative widely studied regularizer is the graph total variation (GTV) and its variants [18–20], which penalize the ℓ_1 norm of edge differences. Since large differences across unreliable edges do not dominate the regularization term as strongly as in the quadratic Laplacian case, GTV can be seen as more robust to edge weight uncertainties. However, this robustness comes at a cost: even on trustworthy edges where the signal should remain smooth, GTV often leaves behind small bumps, making it less effective than Laplacian regularization when the edge weights are accurate.

This naturally leads to the following research ques-

tion: *Can we design a regularization method that recovers the effectiveness of GLR when edge weights are accurate, while significantly improving robustness in the presence of edge weight uncertainties?*

To address this question, we propose a novel regularization framework for graph signal recovery based on infimal convolution. The contributions of this work are summarized as follows:

- We introduce an infimal convolution-based regularizer that combines the strengths of GLR and GTV. The key mechanism is as follows: when an edge weight is reliable, the difference between the graph signal values at its endpoints tends to be small, in which case the ℓ_2 evaluation yields a smaller function value. Conversely, when an edge weight is unreliable, the difference across its endpoints is likely to be relatively large, making the ℓ_1 evaluation more favorable. As a result, the proposed regularizer automatically delegates smoothing to the ℓ_2 component on trustworthy edges, while relying on the ℓ_1 component for edges with uncertainties.

- We formulate general graph signal recovery problems as convex optimization problems incorporating the proposed regularizer, and develop an efficient solver based on a preconditioned primal-dual splitting method [21, 22].

Through experiments on graph signal recovery with perturbed edge weights, we demonstrate that the proposed regularizer exhibits significantly more robust behavior than GLR and GTV under edge weight uncertainties.

2 Preliminaries

2.1 Notations and Definitions

Vectors are denoted by bold lowercase letters, with the i-th element of a vector $\mathbf{x}$ as x_i. Matrices are denoted by bold uppercase letters, with the transpose of a matrix $\mathbf{X}$ as $\mathbf{X}^\top$. Linear operators are denoted by calligraphic uppercase letters, with the adjoint of a linear operator $\mathcal{L}$ as $\mathcal{L}^*$. The set of all proper lower semicontinuous convex functions over $\mathbb{R}^m$ is denoted by $\Gamma_0(\mathbb{R}^m)$. The ℓ_p-norm of a vector $\mathbf{x} \in \mathbb{R}^m$ is defined as $\|\mathbf{x}\|_p = (\sum_i |x_i|^p)^{1/p} \in \Gamma_0(\mathbb{R}^m)$ for $p \geq 1$, and the operator norm of a linear operator $\mathcal{L}$ is defined as $\|\mathcal{L}\|_{\mathrm{op}} = \sup_{\mathbf{x} \neq 0} \|\mathcal{L}\mathbf{x}\|_2 / \|\mathbf{x}\|_2$. The indicator function $\iota_C \in \Gamma_0(\mathbb{R}^m)$ of a set $C \subseteq \mathbb{R}^m$ is defined as $\iota_C(\mathbf{x}) = 0$ if $\mathbf{x} \in C$ and $+\infty$ otherwise. The proximity operator $\mathrm{prox}_{\gamma f}(\mathbf{x}) \colon \mathbb{R}^m \to \mathbb{R}^m$ of a function $f \in \Gamma_0(\mathbb{R}^m)$ with a parameter $\gamma > 0$ is defined as

$$\mathrm{prox}_{\gamma f}(\mathbf{x}) = \underset{\mathbf{y}}{\mathrm{argmin}} \quad f(\mathbf{y}) + \frac{1}{2\gamma}\|\mathbf{y} - \mathbf{x}\|_2^2. \quad (1)$$

We call a function proximable if its proximity operator has a closed form solution or can be efficiently computed.

2.2 Basic Tools in GSP

We consider an undirected weighted graph $G = (V, E, \mathbf{W})$ without self-loops, where $V = \{v_1, \ldots, v_{|V|}\}$ is the set of $|V|$ vertices, $E = \{e_{i,j} = (v_i, v_j)\}$ is the set of $|E|$ edges defined for some $i < j$, and $\mathbf{W} \in \mathbb{R}^{|E| \times |E|}$ is a diagonal matrix collecting weights $w_{i,j} > 0$ associated with $e_{i,j}$. The G can be characterized by its (unnormalized) graph Laplacian $\mathbf{L} = \mathbf{D}^\top \mathbf{W} \mathbf{D} \in \mathbb{R}^{|V| \times |V|}$, with the oriented incidence matrix $\mathbf{D} \in \mathbb{R}^{|E| \times |V|}$ defined by

$$\mathbf{D}_{e_{i,j}, v_k} \coloneqq \begin{cases} -1, & \text{if } i = k, \\ 1, & \text{if } j = k, \\ 0, & \text{otherwise.} \end{cases} \quad (2)$$

A graph signal is a vector $\mathbf{x} \in \mathbb{R}^{|V|}$ with x_i defined on a vertex v_i. Two common measures of signal variation on G are

$$\mathbf{x}^\top \mathbf{L} \mathbf{x} = \sum_{i,j} w_{i,j}(x_i - x_j)^2, \quad (3)$$

$$\|\mathbf{W}\mathbf{D}\mathbf{x}\|_1 = \sum_{i,j} w_{i,j}|x_i - x_j|. \quad (4)$$

The first quantity corresponds to *graph Laplacian regularization (GLR)*, which promotes global smoothness of the signal, while the second corresponds to *graph total variation (GTV)*, which promotes piecewise smoothness.

GLR is highly effective when edge weights accurately reflect signal similarity, but it is sensitive to weight inaccuracies. In contrast, GTV is more robust to uncertain edges since large discrepancies across unreliable connections do not dominate the regularization term. However, this robustness comes at the expense of under-penalizing small but meaningful differences on reliable edges, limiting its effectiveness compared with GLR.

2.3 Infimal Convolution

The infimal convolution [23] of two functions $f, g \in \Gamma_0(\mathbb{R}^d)$ is the function $f \square g \in \Gamma_0(\mathbb{R}^d)$ defined by

$$(f \square g)(\mathbf{u}) = \inf_{\mathbf{C}\mathbf{u} = \mathbf{p} + \mathbf{q}} f(\mathbf{p}) + g(\mathbf{q}), \quad (5)$$

where $\mathbf{C}$ can be any matrix.[1] Intuitively, the infimal convolution finds the optimal separation of the input $\mathbf{C}\mathbf{u}$ into two components $\mathbf{p}$ and $\mathbf{q}$ by automatically balancing their contributions, which are characterized by f and g. This perspective has been incorporated in several regularization designs to capture latent properties without

---

[1] We introduce the matrix $\mathbf{C}$ for generality, whereas the original definition only considers the case where $\mathbf{C}$ is the identity matrix.

requiring prior knowledge of their relative magnitudes. For instance, the total generalized variation (TGV) [24] and its extension to graph signals [19] employ infimal convolution of the first- and second-order total variation (TV) terms.

2.4 Preconditioned Primal-Dual Splitting (P-PDS)

P-PDS [21] can solve convex problems in the form:

$$
\min_{\mathbf{x}_i, \mathbf{y}_j} \quad \sum_{i=1}^{N} f_i(\mathbf{x}_i) + \sum_{j=1}^{M} g_j(\mathbf{y}_j)
$$

$$
\text{s.t.} \quad \forall j \in \{1, \ldots, M\}, \ \mathbf{y}_j = \sum_{i=1}^{N} \mathcal{L}_{j,i}(\mathbf{x}_i), \tag{6}
$$

where $f_i \in \Gamma_0(\mathbb{R}^{n_i})$ and $g_j \in \Gamma_0(\mathbb{R}^{m_j})$ are proximable, and $\mathcal{L}_{j,i} \colon \mathbb{R}^{n_i} \to \mathbb{R}^{m_j}$ are bounded. This algorithm alternates between updating the primal variables $\mathbf{x}_i$ and the dual variables $\mathbf{z}_j$, which are associated with the equality constraint on $\mathbf{y}_j$. The sequence of the updated variables converges to the primal-dual solution of Problem (6) with appropriate stepsizes. A recent study [22] proposed three variable-wise stepsize designs based on the (upper bound of) operator norms $\|\mathcal{L}_{j,i}\|_{\mathrm{op}}$ that guarantee the convergence, with a practical advantage of fast convergence. Let $\rho_i, \gamma_j > 0$ be the stepsizes for $\mathbf{x}_i$ and $\mathbf{z}_j$ determined by this method, respectively. Then, P-PDS iterates the following updates, with an intermediate variable $\widetilde{\mathbf{z}}_j$:

$$
\left\lfloor
\begin{array}{l}
\mathbf{x}_i^{(n+1)} = \mathrm{prox}_{\rho_i f_i}(\mathbf{x}_i^{(n)} - \rho_i \sum_{j=1}^{M} \mathcal{L}_{j,i}^*(\mathbf{z}_j^{(n)})), \\
\widetilde{\mathbf{z}}_j = \mathbf{z}_j^{(n)} + \gamma_j \sum_{i=1}^{N} \mathcal{L}_{j,i}(2\mathbf{x}_i^{(n+1)} - \mathbf{x}_i^{(n)}), \\
\mathbf{z}_j^{(n+1)} = \widetilde{\mathbf{z}}_j - \gamma_j \mathrm{prox}_{\gamma_j^{-1} g_j}(\gamma_j^{-1} \widetilde{\mathbf{z}}_j).
\end{array}
\right. \tag{7}
$$

3 Proposed Method

We now introduce a regularization framework that promotes signal smoothness on the underlying true graph while mitigating the adverse effects of edge weight uncertainties. Based on this design, we formulate graph signal recovery as a convex optimization problem and develop an efficient algorithm to solve it using P-PDS.

3.1 Regularization Design

Our goal is to design a regularizer that inherits the advantages of both GLR and GTV while mitigating their individual limitations. To this end, we leverage the infimal convolution of an ℓ_2 (GLR-like) term and an ℓ_1 (GTV-like) term. The intuition is that reliable edges, where endpoint differences are small, are naturally handled by the ℓ_2 term, whereas unreliable edges, where differences are relatively large, are better absorbed by the ℓ_1 term. This mechanism allows the regularizer to automatically adapt to the reliability of edge weights.

We instantiate this idea in two variants:

$$
\min_{\sqrt{\mathbf{W}} \mathbf{D} \mathbf{u} = \mathbf{p} + \mathbf{q}} \quad \alpha \|\mathbf{p}\|_1 + (1-\alpha)\|\mathbf{q}\|_2^2, \tag{8}
$$

$$
\min_{\mathbf{W} \mathbf{D} \mathbf{u} = \mathbf{p} + \mathbf{q}} \quad \alpha \|\mathbf{p}\|_1 + (1-\alpha)\|\mathbf{D}^\top \mathbf{q}\|_2, \tag{9}
$$

where $\alpha \in [0,1]$ controls the balance between the two components.

The first form (8) retains the exact GLR in its second term, while its first term resembles GTV but only partially incorporates $\sqrt{\mathbf{W}}$. The second form (9) recovers GTV in its first term, whereas its second term imitates GLR in a modified form. We later investigate the impact of these design differences in the experiments.

It is important to note that the above two forms are not equivalent to a simple convex linear combination of GLR and GTV. In a linear combination, the regularization takes the form

$$
\alpha \cdot \mathrm{GLR}(u) + (1-\alpha) \cdot \mathrm{GTV}(u),
$$

where each edge difference contributes simultaneously to both terms. In contrast, the infimal convolution finds an optimal decomposition $\mathbf{p} + \mathbf{q}$ such that *each edge contribution is adaptively assigned* to either the ℓ_1 or the ℓ_2 component. This separation enables edge-wise robustness, a property fundamentally different from globally weighted sums.

For convenience, we express both variants in the following unified form

$$
\min_{\mathbf{B} \mathbf{u} = \mathbf{p} + \mathbf{q}} \quad \alpha \|\mathbf{p}\|_1 + \beta g(\mathbf{A}\mathbf{q}), \tag{10}
$$

where $\beta = 1 - \alpha$. This reduces to (8) when $\mathbf{B} = \sqrt{\mathbf{W}}\mathbf{D}$, $\mathbf{A} = \mathbf{I}$, and $g(\cdot) = \|\cdot\|_2^2$, and to (9) when $\mathbf{B} = \mathbf{W}\mathbf{D}$, $\mathbf{A} = \mathbf{D}^\top$, and $g(\cdot) = \|\cdot\|_2$.

3.2 Problem Statement

We consider the recovery of an underlying smooth graph signal $\overline{\mathbf{u}} \in \mathbb{R}^{|V|}$ from a noisy and possibly incomplete observation $\mathbf{v}$. The observation model is

$$
\mathbf{v} = \mathbf{\Phi}\overline{\mathbf{u}} + \mathbf{n}, \tag{11}
$$

where $\mathbf{\Phi} \in \mathbb{R}^{K \times |V|}$ is a linear observation matrix and $\mathbf{n} \in \mathbb{R}^K$ denotes additive Gaussian noise.

Incorporating the unified regularization in (10), we formulate the recovery problem as the following constrained convex optimization:

$$
\min_{\mathbf{B}\mathbf{u} = \mathbf{p} + \mathbf{q}} \quad \alpha \|\mathbf{p}\|_1 + \beta g(\mathbf{A}\mathbf{q})
$$

$$
\text{s.t.} \quad \mathbf{u} \in R_{\underline{\mu}, \overline{\mu}}, \ \mathbf{\Phi}\mathbf{u} \in B_{\mathbf{v}, r}, \tag{12}
$$

with the closed convex constraint sets

$$R_{\underline{\mu},\overline{\mu}} := \{\mathbf{u} \in \mathbb{R}^{|V|} \mid \underline{\mu} \leq u_i \leq \overline{\mu}\}, \tag{13}$$

$$B_{\mathbf{v},r} := \{\mathbf{z} \in \mathbb{R}^K \mid \|\mathbf{z} - \mathbf{v}\|_2 \leq r\}. \tag{14}$$

The set $R_{\underline{\mu},\overline{\mu}}$ imposes box constraints reflecting prior knowledge of feasible signal ranges (or can be chosen sufficiently wide if such knowledge is unavailable). The set $B_{\mathbf{v},r}$ enforces fidelity to the observations within an ℓ_2 ball of radius $r \geq 0$ centered at $\mathbf{v}$. Such constrained formulations are known to improve robustness and facilitate principled hyperparameter control [25–29].

3.3 Optimiazation Algorithm

We develop an efficient algorithm for solving the proposed convex optimization (12) based on P-PDS with automatic stepsize selection. First, by eliminating $\mathbf{q}$ and introducing the indicator functions of $R_{\underline{\mu},\overline{\mu}}$ and $B_{\mathbf{v},r}$, Problem (12) can be reformulated as

$$\min_{\mathbf{u},\mathbf{p}} \iota_{R_{\underline{\mu},\overline{\mu}}}(\mathbf{u}) + \iota_{B_{\mathbf{v},r}}(\mathbf{\Phi}\mathbf{u}) + \alpha\|\mathbf{p}\|_1 + \beta g(\mathbf{AB}\mathbf{u} - \mathbf{Ap}). \tag{15}$$

Then, by introducing auxiliary variables $\mathbf{y}_1$ and $\mathbf{y}_2$ to separate the composite matrices, it can be equivalently written as

$$\min_{\mathbf{u},\mathbf{p}} \iota_{R_{\underline{\mu},\overline{\mu}}}(\mathbf{u}) + \iota_{B_{\mathbf{v},r}}(\mathbf{y}_1) + \alpha\|\mathbf{p}\|_1 + \beta g(\mathbf{y}_2)$$
$$\text{s.t. } \mathbf{y}_1 = \mathbf{\Phi}\mathbf{u}, \quad \mathbf{y}_2 = \mathbf{AB}\mathbf{u} - \mathbf{Ap}. \tag{16}$$

This formulation reduces to the form in Problem (12) by setting $\mathbf{x}_1 = \mathbf{u}$, $\mathbf{x}_2 = \mathbf{p}$, $f_1 = \iota_{R_{\underline{\mu},\overline{\mu}}}$, $f_2 = \iota_{B_{\mathbf{v},r}}$, $f_3 = \alpha\|\cdot\|_1$, $f_4 = \beta g(\cdot)$, $\mathcal{L}_{1,1} = \mathbf{\Phi}$, $\mathcal{L}_{2,1} = \mathbf{AB}$, and $\mathcal{L}_{2,2} = \mathbf{A}$. All the functions are proper lower-semicontinuous convex and proximable, with the proximity operators:

$$[\text{prox}_{\gamma\iota_{R_{\underline{\mu},\overline{\mu}}}}(\mathbf{x})]_i = \max(\underline{\mu},\ \min(\overline{\mu},\ x_i)), \tag{17}$$

$$\text{prox}_{\gamma\iota_{B_{\mathbf{v},r}}}(\mathbf{x}) = \mathbf{v} + \frac{\min(r,\ \|\mathbf{x} - \mathbf{v}\|_2)}{\|\mathbf{x} - \mathbf{v}\|_2}(\mathbf{x} - \mathbf{v}), \tag{18}$$

$$[\text{prox}_{\gamma\alpha\|\cdot\|_1}(\mathbf{x})]_i = \text{sign}(x_i) \cdot \max(|x_i| - \gamma\alpha,\ 0), \tag{19}$$

$$\text{prox}_{\gamma\beta\|\cdot\|_2}(\mathbf{x}) = (1 - \frac{\gamma\beta}{\max(\|\mathbf{x}\|_2,\ \gamma\beta)})\mathbf{x}, \tag{20}$$

$$\text{prox}_{\gamma\beta\|\cdot\|_2^2}(\mathbf{x}) = \frac{1}{1 + 2\gamma\beta}\mathbf{x}, \tag{21}$$

where $[\cdot]_i$ denotes the i-th element of the outputs and $\text{sign}(u_i)$ is 1 for $u_i \geq 0$ and -1 otherwise. All the linear operators are real matrices and thus bounded, where their operator norms can be calculated as the maximum singular values. Consequently, Problem (12) can be solved by applying P-PDS, enjoying the automatic stepsize designs among the three frameworks mentioned earlier. The detailed flow of this algorithm is summarized in Algorithm 1.

Algorithm 1: P-PDS-based algorithm for solving Problem (12)

Input: $\mathbf{u}^{(0)}, \mathbf{p}^{(0)}, \mathbf{z}_1^{(0)}, \mathbf{z}_2^{(0)}$
while *Stopping criteria are not met* **do**
$\quad \mathbf{u}^{(n+1)} \leftarrow$
$\quad\quad \text{prox}_{\rho_1\iota_{R_{\underline{\mu},\overline{\mu}}}}(\mathbf{u}^{(n)} - \rho_1(\mathbf{\Phi}^\top\mathbf{z}_1^{(n)} + (\mathbf{B}^\top\mathbf{A}^\top)\mathbf{z}_2^{(n)}));$
$\quad \mathbf{p}^{(n+1)} \leftarrow \text{prox}_{\rho_2\alpha\|\cdot\|_1}(\mathbf{p}^{(n)} + \rho_2\mathbf{A}^\top\mathbf{z}_2^{(n)});$
$\quad \widetilde{\mathbf{z}_1} \leftarrow \mathbf{z}_1^{(n)} + \gamma_1\mathbf{\Phi}(2\mathbf{u}^{(n+1)} - \mathbf{u}^{(n)});$
$\quad \mathbf{z}_1^{(n+1)} \leftarrow \widetilde{\mathbf{z}_1} - \gamma_1\text{prox}_{\gamma_1^{-1}\iota_{B_{\mathbf{v},r}}}(\gamma_1^{-1}\widetilde{\mathbf{z}_1});$
$\quad \widetilde{\mathbf{z}_2} \leftarrow$
$\quad\quad \mathbf{z}_2^{(n)} + \gamma_2(\mathbf{AB}(2\mathbf{u}^{(n+1)} - \mathbf{u}^{(n)}) - \mathbf{A}(2\mathbf{p}^{(n+1)} - \mathbf{p}^{(n)}));$
$\quad \mathbf{z}_2^{(n+1)} \leftarrow \widetilde{\mathbf{z}_2} - \gamma_2\text{prox}_{\gamma_2^{-1}g}(\gamma_2^{-1}\widetilde{\mathbf{z}_2});$
$\quad n \leftarrow n + 1;$
Output: $\mathbf{u}^{(n)}$

---

4 Experiments

In this section, we demonstrate the robustness of the proposed regularizations against inaccurate graph weights through graph signal denoising and inpainting performance, compared with GLR and GTV.

4.1 Setup

We experimented with a sensor graph with 64 vertices and 236 edges provided in GSPBox [30], where the weights were synthesized to construct the true and corrupted graphs, then scaled so that the mean was 1. The true weights were generated by deflating uniform weights by 0.1 at randomly selected 50% of edges, and the corrupted weights were generated by reversing these binary weights at randomly selected 10% of edges. The ground-truth smooth signal $\overline{\mathbf{u}}$ was constructed from the low-frequency components of the true graph: the eigenvectors corresponding to the smallest eigenvalues of the graph Laplacian matrix, which give the smallest values of the GLR penalty (3). Specifically, 30% of the low-frequency components were combined with the coefficients drawn from the Gaussian distribution with the standard deviation 1, and then shifted and scaled to the range $[0, 1]$. The box constraint was accordingly set with $\underline{\mu} = 0$ and $\overline{\mu} = 1$. The observation matrix $\mathbf{\Phi}$ was set to a mask on randomly selected 20% of elements for inpainting and an identity matrix for denoising, and the Gaussian noise with the standard deviation 0.05 was added to the non-masked elements. The fidelity constraint was set with $r = 0.9 \cdot 0.05\sqrt{m}$, with m as the number of non-masked elements.

We found the best performance of the proposed regularizations over the balancing parameters $\alpha \in [0, 1]$ through a grid search with the stride 0.005 excluding 0 and 1. The performances of GLR and GTV were ob-

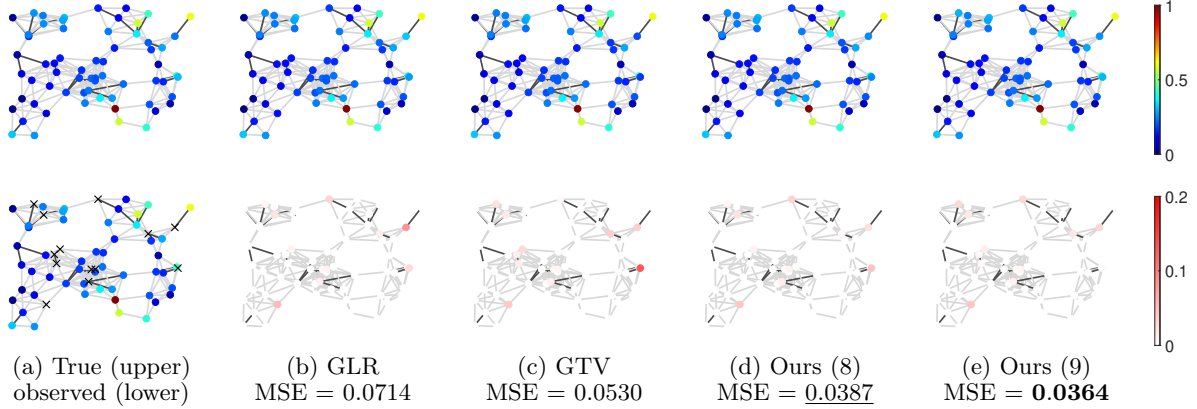| (a) True (upper) observed (lower) | (b) GLR MSE = 0.0714 | (c) GTV MSE = 0.0530 | (d) Ours (8) MSE = 0.0387 | (e) Ours (9) MSE = **0.0364** |

Figure 1: Visual results and NMSEs in one run of noiseless inpainting, where the edges with corrupted weights are highlighted in thicker black. The first column shows the true signal (upper) and the observed signal (lower), with the masked signal elements as cross symbols. In the remaining columns, the first row shows the recovered signals, and the second row highlights the error between the true and restored signals. The proposed regularizations improved the recovery accuracy on nodes where GLR and GTV failed, demonstrating that they successfully inherited different strengths from GLR and GTV.

Table 1: RMSEs averaged over 20 independent runs, with the best and the second best performance highlighted by bolded and underlined, respectively. Our proposed regularizations consistently achieved better performances over GLR and GTV.

Task	GLR	GTV	Ours (8)	Ours (9)
Denoising	0.1757	0.1640	<u>0.1629</u>	**0.1485**
Inpainting	0.1714	0.1848	<u>0.1697</u>	**0.1353**
+ noise	0.2549	0.2637	<u>0.2500</u>	**0.2300**

served with the same formulation and algorithm as the proposed methods, where $\mathbf{p}$ and the balancing parameter were no longer needed. All optimizations were performed with the initial variables set to $\mathbf{0}$ and the stopping criterion set to $\|\mathbf{u}^{(n+1)} - \mathbf{u}^{(n)}\|_{\text{P-PDS}} < 10^{-9}$, where $\|\cdot\|_{\text{P-PDS}}$ is the norm equipped in the primal-dual space of P-PDS [31]. We evaluated the recovery performance by the (normalized) root mean squared error (RMSE) between the true signal $\bar{\mathbf{u}}$ and the recovered signal $\mathbf{u}$: RMSE = $\|\mathbf{u} - \bar{\mathbf{u}}\|_2 / \|\bar{\mathbf{u}}\|_2$, with the lower values indicating better performance.

4.2 Results and Discussion

Table 1 shows the RMSEs averaged over 20 independent runs on each task and regularization, with the best and second best performance highlighted by bolded and underlined, respectively. Our proposed regularizations surpassed GLR and GTV across all tasks, validating their robust smoothness-promoting ability over GLR against inaccurate graph weights. In particular, the pro-

posed method (9) consistently achieved the best performance, which implies the importance of incorporating the exact GTV in the error-tolerant term.

Fig. 1 visualizes an example of recovery results on each method in the noiseless inpainting task, where the edges with corrupted weights are highlighted in thicker black. The first column shows the true signal in the upper and the observed signal in the lower, with the masked signal elements as cross symbols. In the other columns, the first row shows the recovered signals, and the second row highlights the error between the true and restored signals. This figure illustrates the assumptions that inspired our regularization design: GLR and GTV failed on different nodes, indicating their complementary advantages against weight errors. Our proposed regularizations successfully inherited these strengths, as they accurately restored the signal on nodes where GLR and GTV struggled.

5 Conclusion

We proposed an infimal convolution-based regularization framework to address the sensitivity of graph Laplacian regularization (GLR) to edge weight uncertainties. By adaptively separating edge differences into an ℓ_2 or an ℓ_1 component, our method inherits the strengths of both GLR and graph total variation (GTV) while avoiding their weaknesses. Formulated as a convex optimization problem and solved via preconditioned primal-dual splitting, the approach achieves robust recovery over GLR and GTV under perturbed graphs, highlighting the benefit of edge-wise adaptivity.

REFERENCES

[1] D. I. Shuman, S. K. Narang, P. Frossard, A. Ortega, and P. Vandergheynst, "The emerging field of signal processing on graphs: Extending high-dimensional data analysis to networks and other irregular domains," *IEEE Signal Processing Magazine*, vol. 30, no. 3, pp. 83–98, 2013.

[2] A. Sandryhaila and J. M. Moura, "Discrete signal processing on graphs," *IEEE Transactions on Signal Processing*, vol. 61, no. 7, pp. 1644–1656, 2013.

[3] A. Ortega, P. Frossard, J. Kovacevi'c, J. M. Moura, and P. Vandergheynst, "Graph signal processing: Overview, challenges, and applications," *Proceedings of the IEEE*, vol. 106, no. 5, pp. 808–828, 2018.

[4] G. Leus, A. G. Marques, J. M. Moura, A. Ortega, and D. I. Shuman, "Graph signal processing: History, development, impact, and outlook," *IEEE Signal Processing Magazine*, vol. 40, no. 4, pp. 49–60, 2023.

[5] S. Chen, A. Sandryhaila, J. M. Moura, and J. Kovacevi'c, "Signal recovery on graphs: Variation minimization," *IEEE Transactions on Signal Processing*, vol. 63, no. 17, pp. 4609–4624, 2015.

[6] M. Onuki, S. Ono, M. Yamagishi, and Y. Tanaka, "Graph signal denoising via trilateral filter on graph spectral domain," *IEEE Transactions on Signal and Information Processing over Networks*, vol. 2, no. 2, pp. 137–148, 2016.

[7] K. Qiu, X. Mao, X. Shen, X. Wang, T. Li, and Y. Gu, "Time-varying graph signal reconstruction," *IEEE Journal of Selected Topics in Signal Processing*, vol. 11, no. 6, pp. 870–883, 2017.

[8] S. Chen, Y. C. Eldar, and L. Zhao, "Graph unrolling networks: Interpretable neural networks for graph signal denoising," *IEEE Transactions on Signal Processing*, vol. 69, pp. 3699–3713, 2021.

[9] F. Chen, G. Cheung, and X. Zhang, "Manifold graph signal restoration using gradient graph laplacian regularizer," *IEEE Transactions on Signal Processing*, vol. 72, pp. 744–761, 2024.

[10] E. Yamagata, K. Naganuma, and S. Ono, "Robust time-varying graph signal recovery for dynamic physical sensor network data," *IEEE Transactions on Signal and Information Processing over Networks*, vol. 11, pp. 59–70, 2025.

[11] R. Merris, "Laplacian matrices of graphs: a survey," *Linear algebra and its Applications*, vol. 197, pp. 143–176, 1994.

[12] R. Ando and T. Zhang, "Learning on graph with laplacian regularization," *Advances in neural information processing systems*, vol. 19, 2006.

[13] J. Pang and G. Cheung, "Graph laplacian regularization for image denoising: Analysis in the continuous domain," *IEEE Transactions on Image Processing*, vol. 26, no. 4, pp. 1770–1785, 2017.

[14] Y. Zhang, Y. Feng, X. Liu, D. Zhai, X. Ji, H. Wang, and Q. Dai, "Color-guided depth image recovery with adaptive data fidelity and transferred graph laplacian regularization," *IEEE Transactions on Circuits and Systems for Video Technology*, vol. 30, no. 2, pp. 320–333, 2019.

[15] C. Dinesh, G. Cheung, and I. V. Baji'c, "Point cloud denoising via feature graph laplacian regularization," *IEEE Transactions on Image Processing*, vol. 29, pp. 4143–4158, 2020.

[16] P. L. Combettes and J.-C. Pesquet, *Proximal splitting methods in signal processing*, Springer, 2011.

[17] N. Parikh, S. Boyd, et al., "Proximal algorithms," *Foundations and Trends® in Optimization*, vol. 1, no. 3, pp. 127–239, 2014.

[18] S. Chen, A. Sandryhaila, G. Lederman, Z. Wang, J. M. Moura, P. Rizzo, J. Bielak, J. H. Garrett, and J. Kovacevic, "Signal inpainting on graphs via total variation minimization," in *2014 IEEE International Conference on Acoustics, Speech and Signal Processing (ICASSP)*. IEEE, 2014, pp. 8267–8271.

[19] S. Ono, I. Yamada, and I. Kumazawa, "Total generalized variation for graph signals," in *2015 IEEE International Conference on Acoustics, Speech and Signal Processing (ICASSP)*. IEEE, 2015, pp. 5456–5460.

[20] P. Berger, G. Hannak, and G. Matz, "Graph signal recovery via primal-dual algorithms for total variation minimization," *IEEE Journal of Selected Topics in Signal Processing*, vol. 11, no. 6, pp. 842–855, 2017.

[21] T. Pock and A. Chambolle, "Diagonal preconditioning for first order primal-dual algorithms in convex optimization," in *2011 International Conference on Computer Vision*. IEEE, 2011, pp. 1762–1769.

[22] K. Naganuma and S. Ono, "Variable-wise diagonal preconditioning for primal-dual splitting: Design and applications," *IEEE Transactions on Signal Processing*, vol. 71, pp. 3281–3295, 2023.

[23] H. H. Bauschke and P. L. Combettes, *Convex Analysis and Monotone Operator Theory in Hilbert Spaces*, Springer Publishing Company, Incorporated, 2nd edition, 2017.

[24] K. Bredies, K. Kunisch, and T. Pock, "Total generalized variation," *SIAM Journal on Imaging Sciences*, vol. 3, no. 3, pp. 492–526, 2010.

[25] M. V. Afonso, J. M. Bioucas-Dias, and M. A. Figueiredo, "An augmented lagrangian approach to the constrained optimization formulation of imaging inverse problems," *IEEE Transactions on Image Processing*, vol. 20, no. 3, pp. 681–695, 2010.

[26] S. Ono and I. Yamada, "Signal recovery with certain involved convex data-fidelity constraints," *IEEE Transactions on Signal Processing*, vol. 63, no. 22, pp. 6149–6163, 2015.

[27] G. Chierchia, N. Pustelnik, J.-C. Pesquet, and B. Pesquet-Popescu, "Epigraphical projection and proximal tools for solving constrained convex optimization problems," *Signal, Image and Video Processing*, vol. 9, no. 8, pp. 1737–1749, 2015.

[28] S. Ono, "Primal-dual plug-and-play image restoration," *IEEE Signal Processing Letters*, vol. 24, no. 8, pp. 1108–1112, 2017.

[29] S. Ono, "L_0 gradient projection," *IEEE Transactions on Image Processing*, vol. 26, no. 4, pp. 1554–1564, 2017.

[30] N. Perraudin, J. Paratte, D. Shuman, L. Martin, V. Kalofolias, P. Vandergheynst, and D. K. Hammond, "Gspbox: A toolbox for signal processing on graphs," *arXiv preprint arXiv:1408.5781*, 2014.

[31] A. Chambolle and T. Pock, "A first-order primal-dual algorithm for convex problems with applications to imaging," *Journal of Mathematical Imaging and Vision*, vol. 40, no. 1, pp. 120–145, 2011.